

roughly of order unity. We have, however, neglected local self-energy effects by using for the spectral function its value in the bulk liquid instead of that near the surface.

The problem remains to calculate $t_{qp}^{\uparrow\uparrow}$ from microscopic theory. Preliminary results for this function, which have been obtained¹⁵ from the Bogoliubov theory of superfluidity, indicate that t increases monotonically from zero for evaporation energy $E=0$ to a value of order unity for $E/k_B \approx 1$ K. However, the Bogoliubov approximation with δ -function pseudopotential does not give a roton minimum, so that a more realistic treatment is required for the evaporation problem.

It would be valuable to obtain both absolute and angular distribution measurements of the evaporating current. An equally crucial and difficult measurement is that of scattering by the liquid surface of a beam of He atoms. This experiment can yield detailed information about both elastic and inelastic processes occurring at the He surface.

The author is grateful to Professor A. Griffin for valuable discussion of this problem. He wishes also to thank Professor D. Goodstein, Professor M. H. Cohen, and Professor R. F. Tinker for helpful comments.

*Work supported in part by the National Research Council of Canada.

¹A. Widom, Phys. Lett. **29A**, 96 (1969).

²P. W. Anderson, Phys. Lett. **29A**, 563 (1969).

³D. S. Hyman, M. O. Scully, and A. Widom, Phys. Rev. **186**, 231 (1969).

⁴A. Griffin, Phys. Lett. **31A**, 222 (1970).

⁵J. I. Kaplan and M. L. Glasser, Phys. Rev. A **3**, 1199 (1971).

⁶J. G. King and W. D. Johnston, Phys. Rev. Lett. **16**, 1191 (1966).

⁷We take $\hbar=1$ throughout.

⁸K. R. Atkins, R. Rosenbaum, and H. Seki, Phys. Rev. **113**, 751 (1959); G. H. Hunter and D. V. Osborne, J. Phys. C: Proc. Phys. Soc., London **2**, 2414 (1969).

⁹L. D. Landau and E. M. Lifshitz, *Statistical Physics* (Pergamon, London, 1958), p. 176.

¹⁰J. G. King, J. McWane, and R. F. Tinker, Bull. Amer. Phys. Soc. **17**, 38 (1972).

¹¹M. H. Cohen, L. M. Falicov, and J. C. Phillips, Phys. Rev. Lett. **8**, 31 (1962).

¹²The broadening of the state, which was considered in Ref. 3, affects the present result negligibly.

¹³J. A. Appelbaum and W. F. Brinkman, Phys. Rev. **186**, 464 (1969).

¹⁴See, e.g., W. L. McMillan and J. M. Rowell, in *Superconductivity*, edited by R. D. Parks (Dekker, New York, 1969), Vol. I.

¹⁵A. Griffin and J. Demers (unpublished) represent the surface by a discontinuity in both real and off-diagonal potentials.

Numerical Simulation on Plasma Diffusion in Three Dimensions*

Hideo Okuda and John M. Dawson

Plasma Physics Laboratory, Princeton University, Princeton, New Jersey 08540

(Received 20 March 1972)

Three-dimensional plasma numerical simulation on cross-field diffusion has been performed for cases with closed and nonclosed field lines of force. For the former case, the diffusion essentially takes the form found for two dimensions showing the three regions of diffusion, while for the latter, the diffusion follows the classical theory to stronger fields. However, the diffusion is always enhanced above the classical level when the magnetic field exceeds a critical value.

Three-dimensional (3D) computer experiments on plasma diffusion have been performed extending the previous 2D and $2\frac{1}{2}$ D calculations.^{1,2} The particle model used was an electrostatic dipole code³ with an external magnetic field \vec{B} . The simulation was carried out in a cubic box of dimensions L^3 with periodic boundary conditions as sketched in Fig. 1. θ and ψ are the angles between the coordinate and the external magnetic field, and they are chosen at the beginning of calculations. Particles were initially distributed uniformly in the box with a Maxwell velocity dis-

tribution. All of the results reported here include the full dynamics of the particles. The diffusion coefficient is measured from the displacement of the guiding centers of a set of test particles [$D_{i,e} = (\Delta r_g)_{i,e}^2 t$].

We find that the cross-field diffusion is always enhanced above the classical level when the magnetic field exceeds a critical value. When the magnetic field is parallel to one of the coordinate axes, say, the z axis, then this corresponds to a system with closed field lines, and enhanced diffusion due to plasma convections associated

with the electric field for modes with $\vec{k} \cdot \vec{B} = 0$ (flute perturbations) occurs. These modes are created by the excess charges contained in the tubes of flux and the charges are not easily dissipated for large \vec{B} . Therefore, the diffusion is similar to the 2D diffusion studied previously.^{1,2} When the magnetic field is not parallel to any of the axes, field lines are not closed, corresponding to a system with a rotational transform. The diffusion follows the classical form up to stronger magnetic fields. This is partly because the plasma convections damp quickly as a result of particle motion along field lines (particles do not stay on the same field lines and therefore the excess charge in a flux tube which is associated with the convection is rapidly neutralized) and partly because a particle sees different phases of the convection as it moves along. However, when the magnetic field is strong enough so that the gyroradii of ions and electrons become smaller than the size of plasma convections whose lifetimes are long compared to the gyroperiods, then convection enhances the diffusion above the classical level. The critical size of plasma convective cells will depend on the strength of the rotational transform and the magnetic shear in real systems.

The classical collision theory⁴ gives the following diffusion coefficients:

$$\frac{D_e}{\omega_{pe}} = \frac{1}{3\sqrt{2}\pi^{3/2}} \frac{\omega_{pe}^2}{\omega_{ce}^2} \frac{1}{n\lambda_D} \ln(\Lambda) \left[1 + \left(\frac{2m_i}{m_i + m_e} \right)^{1/2} \right],$$

$$\frac{D_i}{D_e} = \left(\frac{m_i}{m_e} \right)^{1/2} \frac{1 + [2m_e/(m_i + m_e)]^{1/2}}{1 + [2m_i/(m_i + m_e)]^{1/2}},$$
(1)

where $\ln \Lambda = \ln(KT\lambda_D/e^2)$. Since we are looking at test-particle diffusion, collisions of test ions with background ions or test electrons with background electrons lead to their diffusion, and the ion and the electron diffusion rates need not be equal. However, if one keeps the diffusion due only to ion-electron collisions which are the only terms that dissipate density inhomogeneities,⁴ then it follows that $D_e = D_i$.

Figure 1 shows the results of two different sets of experiments with different angles (θ, ψ) using $\lambda_D = 3$, $m_i/m_e = 1.25$, and $n\lambda_D^3 = 3.5$ (distance is measured in grid spacing). The magnetic field was varied from $\omega_{pe}/\omega_{ce} = 4$ to 0.25. The case $(\theta, \psi) = (0, 0)$ corresponds to a system with closed field lines because particles leaving one boundary will return to the other on the same field line. Classical collision theory as given by Eq. (1) agrees very well with the simulation for ω_{pe}/ω_{ce}

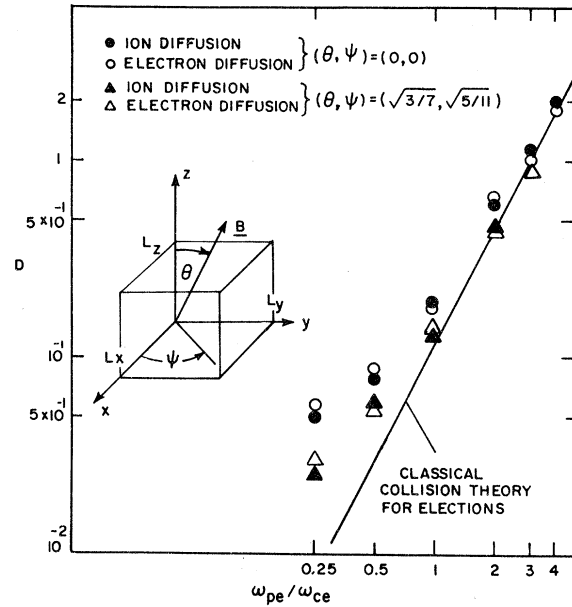


FIG. 1. Two sets of experiments for closed and non-closed field lines in a collisional region. For a weak magnetic field, the collision theory agrees very well. $\lambda_D = 3$, $m_i/m_e = 1.25$, and $n\lambda_D^3 = 3.5$ were used on a $32 \times 32 \times 32$ grid.

≥ 3 . However, for stronger fields, the observed diffusion is several times enhanced above the classical value. The enhancement is due to plasma convections with $\vec{k} \cdot \vec{B} = 0$ and is similar to the 2D situation.^{1,2} A flux tube can acquire an excess charge which is not easily dissipated. The resultant electric field gives rise to plasma convection and hence to plasma diffusion.

The enhanced diffusion can be suppressed to some extent by choosing the angle (θ, ψ) so that there are no modes of the fluctuating field with long wavelength which satisfy $\vec{k} \cdot \vec{B} = 0$. The field lines are no longer closed but more or less fill the volume as they repeatedly cross the system (we could, of course, have magnetic surfaces or ergodic lines or lines which close after a few traversals of the system depending on the angle chosen). In this case local excess charge can

be rapidly dissipated by flow along the lines. This effect is illustrated by choosing the angle $(\theta, \psi) = (\frac{3}{7})^{1/2}, (\frac{5}{11})^{1/2}$ shown by the triangles in Fig. 1. The collision theory fits the simulations precisely up to $\omega_{pe}/\omega_{ce} = 2$; however, there is an enhancement for stronger fields.

Since $n\lambda_D^3 = 3.5$ here, the plasma is rather collisional and the mean free path is about 20 which is smaller than the size of the system ($L = 32$). (The use of finite-size particles increases the effective $n\lambda_D^3$ by a factor of 2.⁵) Therefore, in transiting the system a particle diffuses a few gyroradii, losing its original field line. Under these conditions excess charge on a flux tube is fairly rapidly dissipated by diffusion across B , and this can compete with charge dissipation due to motion along lines of force. This is shown by the fact that the diffusion rate was not reduced below that given by the triangles when other angles (θ, ψ) were chosen.

For a much more collisionless plasma with the mean free path much larger than the system, the effect of the angle is much greater. Any flux tube which has an excess charge on it will retain that charge for a long time since the collisional diffusion will be very slow. The convective motion may distort and stretch out a flux tube (its volume must, of course, be essentially constant)

so that collisional diffusion may more rapidly dissipate the charge. However, for large convective cells this process still takes a long time.

Figure 2 shows the result of two sets of simulation in the collisionless region where $\lambda_D = 5\sqrt{2}$, $m_i/m_e = 1.25$, and $n\lambda_D^3 = 170$. Here, the mean free path is $l \approx 1200$ which is much greater than the size of the system.

For $(\theta, \psi) = (0, 0)$, the simulation points show a diffusion rate much greater than that predicted by the collision theory. This is because the collisional diffusion decreases as $(n\lambda_D^3)^{-1}$ while the diffusion due to convections decreases as $n^{-1/2}$. The enhanced diffusion stays more or less constant with increasing B until $\omega_{pe}/\omega_{ce} = 0.25$, at which point it begins to decrease, following a l/B law. This indicates that the diffusion is mainly due to convections created by the modes with $\vec{k} \cdot \vec{B} = 0$ just as for a 2D model.^{1,2}

The enhanced diffusion is strongly suppressed by choosing $(\theta, \psi) = (\frac{3}{7})^{1/2}, (\frac{5}{11})^{1/2}$ for a collisionless plasma in contrast to the collisional case. For the choice $(\theta, \psi) = (0, 0)$, excess charges stay on the same flux tube for many passes of a particle through the system. However, for a choice of $(\theta, \psi) = (\frac{3}{7})^{1/2}, (\frac{5}{11})^{1/2}$, field lines connect all parts of the system and the motion of particles along field lines rapidly neutralizes local excess charges.

Although a rotational transform and a magnetic shear can strongly suppress the enhanced diffusion due to plasma convections, it is seen from these results (Fig. 2) that for a strong enough field, enhanced diffusion still occurs. When the gyroradii of ions and electrons become less than the size of plasma convective cells with appreciable lifetimes, convection must start to play a role. It appears that convection can explain enhanced diffusion observed in a semiconductor plasma.⁶

Convections of electrons by waves whose frequency exceeds the ion gyrofrequency can lead to their diffusion relative to the ions.² Figure 3 shows results from such a simulation using $\lambda_D = 3$, $m_i/m_e = 400$, and $n\lambda_D^3 = 3.5$. Here, only the electron diffusion was measured. For $\omega_{pe}/\omega_{ce} \geq 2$, the measurements agree well with collision theory, while for stronger fields, a large enhancement is observed. The explanation is as follows: It can be shown that most of the fluctuation electric field energy is in high-frequency electron oscillations such as at the upper hybrid for $\omega_{pe}/\omega_{ce} > 1$, while for $\omega_{pe}/\omega_{ce} < 1$, the energy shifts to low-frequency ion oscillations such as

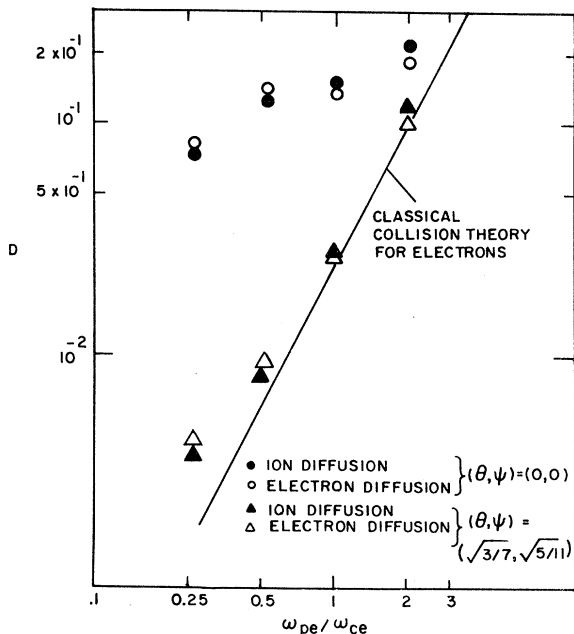


FIG. 2. Two sets of experiments for closed and non-closed field lines in a collisionless region. The enhanced diffusion due to plasma convection is suppressed very effectively for the case of nonclosed field lines. $\lambda_D = 5\sqrt{2}$, $m_i/m_e = 1.25$, and $n\lambda_D^3 = 170$ were used on a $32 \times 32 \times 32$ grid.

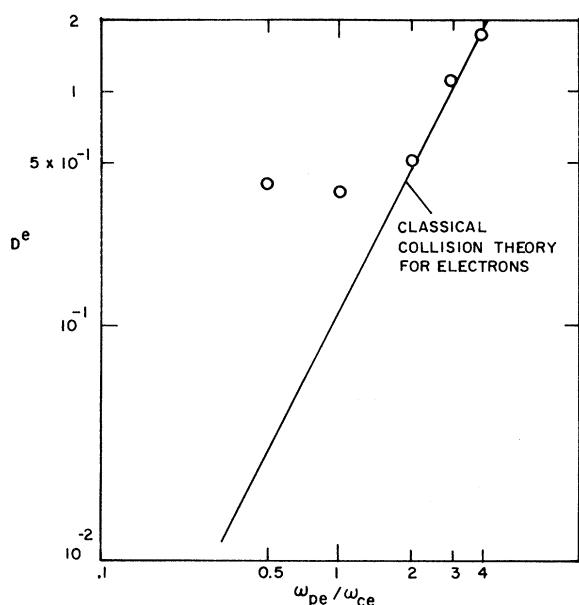


FIG. 3. A set of experiments using a large mass ratio. Only the electron diffusion was measured. $\lambda_D = 3$, $m_i/m_e = 400$, and $n\lambda_D^3 = 3.5$ were used on a $32 \times 32 \times 32$ grid.

the lower-hybrid oscillation and the zero-frequency vortex mode.² It is clear that these oscillations can cause electron convections by $c\vec{E} \times \vec{B}/B^2$ motion but that the ions will not be able to follow if $\omega > \omega_{ci}$.

The following are some theoretical considerations of the convective diffusion.⁷ Let us consider a case with closed field lines. As already pointed out for such a case, tubes of flux can contain excess charges which in turn produce the electric field with $\vec{k} \cdot \vec{B} = 0$. The electric field associated with these charged lines of force gives rise to vortex motions as in the 2D case studied earlier.^{1,2} Following the theory for turbulent diffusion by Weinstock and Williams,⁸ the cross-field diffusion coefficient can be written as

$$D_{\perp} = \frac{2c^2}{B^2} \sum_k (E^2)_k \text{Im} \frac{-1}{\omega + ik_{\perp}^2 D_{\perp} + ik_{\parallel}^2 D_{\parallel}}, \quad (2)$$

where $(E^2)_k$ and ω are the respective field energy and the frequency of mode \vec{k} associated with the plasma convection. For $\omega \approx 0$, $(E^2)_k$ is given by^{1,2}

$$\frac{(E^2)_k}{8\pi} V = \frac{1}{2} K T \frac{1}{1 + \omega_{pi}^2/\omega_{ci}^2 + \omega_{pe}^2/\omega_{ce}^2}, \quad (3)$$

where $V = l_1^2 l_2$, with l_1 and l_2 the lengths of the system across and along magnetic field lines. Substituting Eq. (3) into Eq. (2) and summing over

k with $\vec{k} \cdot \vec{B} = 0$, one finds

$$D_{\perp} = 2^{3/2} \frac{c}{B} \left(\frac{KT \ln l_1 k_{\max}}{(1 + \omega_{pi}^2/\omega_{ci}^2 + \omega_{pe}^2/\omega_{ce}^2) l_2} \right)^{1/2}; \quad (4)$$

k_{\max} is the largest allowed wave number perpendicular to \vec{B} . Equation (4) gives Bohm-type diffusion ($D_{\perp} \propto l/B$) when $\omega_{pi}^2/\omega_{ci}^2 < 1$. When $\omega_{pi}^2/\omega_{ci}^2 > 1$, the diffusion is

$$D_{\perp} = \frac{v_{Ti} (\ln l_1 k_{\max})^{1/2}}{[(3\pi/2)nl_2]^{1/2}} \quad (5)$$

which is independent of magnetic field. The flat region in Fig. 2 is close to the value given by Eq. (5).⁹ The ratio of Eq. (5) to Eq. (1) is

$$\frac{D_{\text{convective}}}{D_{\text{collisional}}} = 2\sqrt{3} \pi \left(\frac{m_e}{m_i} \right)^{1/2} \left(n\lambda_D^3 \frac{\lambda_D}{l_2} \right)^{1/2} \times \frac{\omega_{ce}^2}{\omega_{pe}^2} \frac{(\ln l_1 k_{\max})^{1/2}}{\ln \Lambda}. \quad (6)$$

Since $n\lambda_D^3$ is a large number while λ_D/l_2 is a small number, the ratio can be of the order of unity for a wide range of plasma parameters when $\omega_{pe} \approx \omega_{ce}$. For example, the ratio is 10% for the experiment given in Ref. (10) and may explain the enhanced diffusion observed there.

For a case with nonclosed field lines, such as the case shown by triangles in Figs. 1 and 2, it is necessary to use a 3D turbulence theory including such effects as wave-particle interaction and the inductive effects associated with the current along field lines. Work on such a program is now in progress.

*Work jointly supported by U. S. Air Force Office of Scientific Research under Contract No. F44620-70-C-0033 and U. S. Naval Research Laboratory under Contract No. N00014-67-A-0151-0021. Use was made of computer facilities supported in part by National Science Foundation Grant No. NSF-GP579.

¹J. M. Dawson, H. Okuda, and R. N. Carlile, Phys. Rev. Lett. **27**, 491 (1971).

²H. Okuda and J. M. Dawson, Princeton Plasma Physics Laboratory Report No. PPL-AP52 (to be published).

³J. Denavit and W. L. Kruer, Phys. Fluids **14**, 1782 (1971).

⁴C. L. Longmire and M. N. Rosenbluth, Phys. Rev. **103**, 507 (1956).

⁵H. Okuda and C. K. Birdsall, Phys. Fluids **13**, 2123 (1970); also, A. B. Langdon and C. K. Birdsall, Phys. Fluids **13**, 2115 (1970).

⁶M. N. Gurnee, W. M. Hooke, G. J. Goldsmith, and M. H. Brennan, Phys. Rev. A **5**, 158 (1972). A detailed comparison of the real experiment with the simulation

will be reported.

⁷The theory is an extension of that given in Ref. 1, and the details of the theory here are found in Ref. 2.

⁸J. Weinstock and R. H. Williams, *Phys. Fluids* **14**, 1472 (1971).

⁹Here it is not proper to replace the sum over \vec{k} by the integral, since the system is only a few Debye (gyro) lengths across.

¹⁰T. Ohkawa, J. R. Gilleland, T. Tamano, T. Takeda, and D. K. Bhadra, *Phys. Rev. Lett.* **27**, 1179 (1971).

New Method for Measuring the Twist Elastic Constant K_{22}/χ_a and the Shear Viscosity γ_1/χ_a for Nematics

P. E. Cladis

Physique des Solides, Université Paris-Sud, 91-Orsay, France*

(Received 13 March 1972)

By monitoring the change in the interference figure for an oriented nematic (optic axis perpendicular to the incident light cone) as twist deformation is induced by a magnetic field (Freedericksz transition), one is led to a simple and direct method for measuring K_{22}/χ_a and γ_1/χ_a . An analytic expression is obtained for the effect of twist on the interference figure and is verified experimentally.

The interference figure¹ for an oriented nematic (held between rubbed² parallel glass plates), with the director (optic axis) in a plane perpendicular to the axis of the incident light cone, is composed of four more or less equilateral hyperbolas. In 1911, Mauguin³ demonstrated that twisting the top plate with respect to the bottom by an angle α resulted in a simple rotation of the hyperbolas (about an axis perpendicular to the figure) through an angle $\delta = \frac{1}{2}\alpha$. More recently, de Gennes⁴ has remarked (see Appendix) that for any twisted nematic the interference figure would, to a first approximation, rotate by an amount δ , given by

$$\tan 2\delta = \langle \sin 2\theta \rangle / \langle \cos 2\theta \rangle, \quad (1)$$

where $\theta(z)$ is the twist angle of the director and $z = \pm \frac{1}{2}d$ defines the glass-nematic interfaces (inset, Fig. 1). $\sin 2\theta$ and $\cos 2\theta$ are to be averaged over the sample thickness d . Thus, if twist is induced by means of a magnetic field applied in the plane of the plates, but perpendicular to the direction of rubbing (Freedericksz transition) so that $\theta(\pm \frac{1}{2}d) = 0$, but $\theta(z=0) = \theta_m \neq 0$, δ will not be zero and such a deformation would be observable even for relatively small θ_m . It is evident that, because of the boundary conditions and the adiabatic theorem, such a deformation may not be observed by microscopy. Nor can it be observed by monitoring the dielectric constant (or thermal conductivity or any other anisotropic property of a uniaxial nematic), since the director remains in the same plane as the glass plates in both the twisted and untwisted configurations. Consequent-

ly, Eq. (1) represents a simple and new method for quantitatively observing twist deformations in uniaxial liquid crystals.

The purpose of this note is to verify Eq. (1) for the Freedericksz transition and to show that the existence of this effect leads to a new and direct method for detecting this transition and hence for measuring K_{22}/χ_a and γ_1/χ_a , where γ_1 is the shear viscosity, K_{22} the Frank elastic constant of twist, and $\chi_a = \chi_{\parallel} - \chi_{\perp}$ is the diamagnetic anisotropy. It is also shown that the average twist deformation may be quantitatively measured as a function of applied magnetic field.

The critical field H_c for the Freedericksz transition for twist is given by⁵

$$H_c = (\pi/d)(K_{22}/\chi_a)^{1/2}. \quad (2)$$

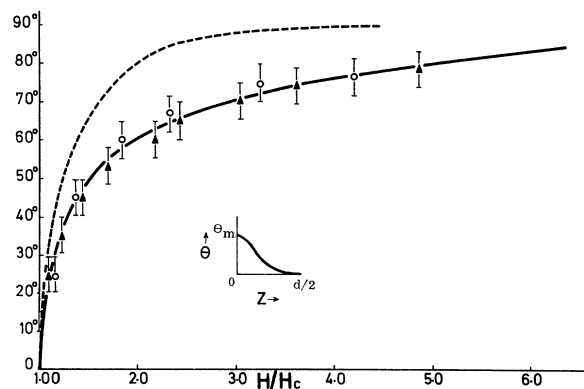


FIG. 1. θ_m , the maximum twist angle for the director, shown as a function of reduced field H/H_c (dashed curve). Solid curve, rotation angle of the interference figure [Eq. (4)]. Experimental points are for MBBA at room temperature.